

QCM-D and Spectroscopic Ellipsometry Measurements of the Lipid Bilayer Anchoring Stability and Kinetics of Hydrophobically Modified DNA Oligonucleotides

Stef A. J. van der Meulen^{†,*}, Galina V. Dubacheva[‡], Marileen Dogterom^{†,§}, Ralf P. Richter^{‡,||,⊥}, and Mirjam E. Leunissen[†]

[†]FOM Institute AMOLF, Science Park 104, 1098 XG, Amsterdam, The Netherlands

[‡]Biosurfaces Unit, CIC biomaGUNE, Paseo Miramon 182, 20009 Donostia-San Sebastian, Spain

[§]Bionanoscience, TU Delft, Lorentzweg 1, 2628 CJ Delft, The Netherlands

^{||}Département de Chimie Moléculaire, Université de Grenoble, BP 53, 38041 Grenoble Cedex 9, France

[⊥]Max-Planck-Institute for Intelligent Systems, Heisenbergstrasse 3, 70569 Stuttgart, Germany

ABSTRACT: The anchoring of DNA oligonucleotides to lipid bilayers through different hydrophobic modifications was studied using quartz crystal microbalance with dissipation monitoring (QCM-D) and spectroscopic ellipsometry (SE). Decorating lipid bilayers with oligonucleotides has great potential for both fundamental studies and applications, taking advantage of the membrane properties and the specific Watson-Crick base pairing. Systematic characterization of the interactions between the DNA and the lipid bilayers remains however limited. We studied the anchoring of oligonucleotides modified with the frequently used hydrophobic anchors cholesterol, stearyl and di-stearyl in the 5' end. All three anchors were found to incorporate well into lipid membranes, yet only the di-stearyl-based anchor remained stable in the bilayer upon rinsing. The unstable anchoring of the cholesterol and stearyl-based oligonucleotides can however be stabilized by hybridization of the oligonucleotides to complementary DNA modified with a second hydrophobic anchor of the same type. In all cases, the incorporation into the lipid bilayer was found to be mass-transport limited, although micelle formation likely reduced the effective concentration of available oligonucleotides in some samples, leading to substantial differences in binding rates. Using a viscoelastic model to determine the thickness of the DNA layer and elucidating the surface coverage by SE, we found that at equal bulk concentrations

double stranded DNA constructs attached to the lipid bilayer establish a thicker layer as compared to the single stranded oligonucleotides, whereas the DNA surface densities are similar. Shortening the length of the oligonucleotides on the other hand does alter both the thickness and surface density of the DNA layer. This indicates that at the bulk oligonucleotide concentrations employed in our experiments, the packing of the oligonucleotides is not affected by the anchor type, but rather by the length of the DNA. The presented results are useful for material and biomedical applications that require efficient linking of oligonucleotides to lipid membranes.

INTRODUCTION

Targeting DNA oligonucleotides to lipid bilayers is an attractive approach to produce new materials, to create highly tunable model systems for studying fundamental questions and for therapeutic applications. Currently, several hydrophobic DNA modifications that mediate the spontaneous anchoring of the oligonucleotides into a lipid bilayer are commercially available. Once the DNA strands are anchored, the specificity of their interaction with complementary DNA sequences can be used for a plethora of purposes.

In the design of anti-sense medicine for example, single-stranded oligonucleotides are targeted to cellular membranes through a hydrophobic moiety, after which they are internalized by the cell allowing the oligonucleotides to hybridize to targeted mRNA strands by sequence recognition and thereby preventing translation of the associated protein.¹⁻³ Lipophilic oligonucleotides are also used in the site-selective immobilization of lipid vesicles to surfaces by linking complementary DNA, incorporated in the lipid bilayer of vesicles on the one hand, and in the planar lipid bilayer on a substrate on the other.⁴⁻⁶ The surface-bound vesicles can then function as miniaturized experimental containers to reduce reagent consumption, monitor fast chemical kinetics, or even to study single molecules. DNA-functionalized vesicles have also been shown to be of great value to study vesicle fusion, or model processes like cell-adhesion and cell-cell interactions.⁷⁻¹⁰ And recently, we used lipophilic DNA to decorate lipid bilayer-coated silica microparticles with specific, surface-mobile binding groups.¹¹ We found that the diffusivity of the binding groups greatly improved the microparticle self-assembly properties.

Most applications require stable incorporation of the oligonucleotides in the lipid bilayer but there still is only limited experimental information on the anchoring characteristics of hydrophobically modified oligonucleotides. Knowledge of the anchoring and kinetics and the organization of oligonucleotides on the surface would provide a better control on functionalization, in particular on the DNA grafting density. We therefore measured the lipid bilayer anchoring characteristics of oligonucleotides with three frequently

used hydrophobic moieties by the surface-sensitive techniques quartz crystal microbalance with dissipation monitoring (QCM-D) and spectroscopic ellipsometry (SE). The combination of these techniques allows us to monitor binding events *in situ* at high temporal resolution without the need for labels and at the same time provides information about the molecular organization within the DNA film.

The anchors that we have investigated are cholesterol (Chol), stearyl (C_{18}) and distearyl (C_{18})₂ of which the chemical structures are shown in Fig. 1a. In addition, we have studied the differences between single versus double stranded DNA, one versus two anchors and made the comparison with shorter oligonucleotides. An overview of all the oligonucleotide types and their hydrophobic terminal modifications included in this study is given in Table. 1 and Fig. 1b.

EXPERIMENTAL METHODS

Materials and Sample Preparation Procedures. We studied the anchoring of hydrophobically modified DNA oligonucleotides to a supported lipid bilayer (SLB), by first forming a lipid bilayer on a planar silica-coated QCM-D sensor and subsequently flowing in the oligonucleotide suspension. To this end, 1,2-dioleoylphosphatidylcholine lipids (DOPC, Avanti Polar Lipids, Alabaster, AL, USA) were dissolved in chloroform and then dried with a gentle stream of $N_2(g)$ and two hours of vacuum desiccation. The dried lipids were subsequently re-suspended to 2 mg/ml in a filtered (pore-size: 0.2 μm) and degassed (30 min) buffer solution of 150 mM NaCl, 10 mM HEPES, pH 7.4, in ultra-pure water and homogenized by repeating five freeze/thaw cycles with liquid nitrogen. Small unilamellar vesicles (SUVs) were formed by sonication (30 min) with a tip sonicator (Branson, USA), operated in pulsed mode at 30% duty cycle with refrigeration, followed by centrifugation in an Eppendorf centrifuge (30 min at 60,000 g) to remove any titanium particles that may possibly be present. SUV suspensions were stored at 4°C under nitrogen. Before assembling a SLB, the vesicle suspensions were diluted to 50

$\mu\text{g}/\text{ml}$ in the aforementioned buffer containing an additional 2 mM CaCl_2 .

After the successful formation of a SLB on the QCM-D sensor, we added the oligonucleotides, see Table 1 and Fig. 1 for an overview of the different types used. The Chol and C_{18} conjugated constructs were synthesized by Eurogentec (Liège, Belgium), and the sequences modified with $(\text{C}_{18})_2$ were produced by ATDBio (Southampton, UK). Upon delivery, the oligonucleotides were dissolved to desired concentrations in the same buffer as mentioned above without CaCl_2 and stored at -20°C . To study the effect of two anchors, or compare single and double stranded DNA bearing only one anchor, some of the sequences in Table 1 were pre-hybridized by mixing equal amounts of two complementary strands and slowly cooling from 90 to 22°C at a rate of $1.5^\circ\text{C}/\text{min}$.

Quartz Crystal Microbalance with Dissipation Monitoring (QCM-D). QCM-D measures the changes in the resonance frequency, Δf , and dissipation, ΔD , of a sensor crystal upon interaction of soft matter with its surface. The QCM-D response is sensitive to the mass (including any hydrodynamically coupled water) and the mechanical properties of the surface-bound layer. To enable SLB formation, we used silica-coated QCM-D sensors (Qsx303; Biolin Scientific, Västra Frölunda, Sweden), which were cleaned in a 2% sodium dodecyl sulfate solution for 30 minutes, rinsed with ultra-pure water, blow-dried with $\text{N}_2(\text{g})$ and exposed to UV/ozone (BioForce Nanosciences, Ames, IA, USA) for 30 minutes prior to usage. The measurements were performed using the Q-Sense E4 system equipped with four Q-Sense Flow Modules (Biolin Scientific). The system was operated in flow mode at a rate of $20 \mu\text{l}/\text{min}$ at 23°C unless stated otherwise. The Δf and ΔD responses at 6 overtones ($i = 3, 5, \dots, 13$, corresponding to resonance frequencies of 15, 25, \dots , 65 MHz) were simultaneously monitored during SLB formation and subsequent DNA binding and unbinding. Throughout this manuscript only changes in dissipation, ΔD_i and normalized frequencies, $\Delta f_i/i$, for $i = 7$ are presented. The oligonucleotides were diluted to $1 \mu\text{M}$ concentrations unless stated otherwise and were added after a proper SLB had formed. We continued the administration of oligonucleotides until saturated binding was reached or for a maximum of 60-75 minutes, after which we rinsed the func-

tionalized SLB with buffer to measure any potential unbinding of the oligonucleotides. The adsorption and desorption of all oligonucleotides were measured two to four times. Representative measurements are presented in the displayed figures.

The thickness and viscoelastic properties of the final DNA film on the SLB were determined by fitting the QCM-D data to a continuum viscoelastic model.^{12–15} The model relates the measured QCM-D responses, Δf and ΔD as a function of i , to the viscoelastic properties of the adsorbed layer and the surrounding solution. The oligonucleotide films were modeled as homogeneous viscoelastic layers with acoustic thickness d , density ρ , storage modulus $G'(f)$, and loss modulus $G''(f)$. The frequency dependence of the storage and loss moduli was assumed to follow power laws, with exponents α' and α'' , respectively. The semi-infinite bulk solution was assumed to be Newtonian with a viscosity of $\eta = 0.89$ mPa·s, and a density of $\rho = 1.0$ g/cm³. Data at selected time points were fitted with the software QTM (D. Johannsmann, Technical University of Clausthal, Germany^{13,14}). Details of the fitting procedure, including the method used to validate the uniqueness of the fit, have been described by Eisele et al.¹⁶

Spectroscopic Ellipsometry (SE). Spectroscopic ellipsometry measures the changes in the ellipsometric angles, Δ and Ψ , of polarized light upon reflection at a planar surface. *In situ* combined QCM-D/SE measurements were performed on QCM-D sensors with a special silica coating (QSX335; Biolin Scientific), using the Q-Sense Ellipsometry Module (Biolin Scientific). The special coating consists of Ti, TiO₂ and SiO₂ layers, where the Ti interlayer is thick enough to be treated as a fully opaque film. The flow module was mounted with the Q-Sense E1 system on a spectroscopic rotating compensator ellipsometer (M2000V, Woollam, NE, USA). Ellipsometric data, Δ and Ψ , were acquired over a wavelength range $\lambda = 380$ to 1000 nm, at 65° angle of incidence. Prior to measurements, we verified that the polarization of the light beam was not affected by the glass windows of the flow chamber as previously described.¹⁷ Measurements were performed in flow mode (20 μ l/min) at 23°C. The oligonucleotides were dissolved to 2 μ M concentration and added in injection mode as described elsewhere.¹⁷

The refractive index ($n(\lambda)$) and optical thickness (d) of the oligonucleotide film were determined by fitting the ellipsometric data to a multilayer model, using the software CompleteEASE (Woollam). The model relates the measured Δ and Ψ as a function of λ to the optical properties of the sensor surface (Ti/TiO₂/SiO₂), the adsorbed films (SLB and oligonucleotide layer), and the surrounding solution. The semi-infinite bulk solution was treated as a transparent Cauchy medium, with a refractive index $n_{\text{sol}}(\lambda) = A_{\text{sol}} + B_{\text{sol}}/\lambda^2$. For the surrounding buffer solution, $A_{\text{sol}} = 1.325$ and $B_{\text{sol}} = 0.00322 \mu\text{m}^2$ were used.¹⁸ The optical properties of the opaque Ti layer were determined from data acquired in air and in the presence of bulk solution by fitting $n_{\text{Ti}}(\lambda)$ and $k_{\text{Ti}}(\lambda)$ over the accessible wavelength range using a B-spline algorithm implemented in CompleteEASE. Simultaneously, thicknesses of the two additional oxide layers (d_{TiO_2}) and (d_{SiO_2}) were fitted assuming them as Cauchy films with tabulated optical constants (n_{TiO_2} from CompleteEASE and n_{SiO_2} from Biolin Scientific). The solvated SLB and oligonucleotide films were treated as separate layers, which we assumed to be transparent and homogeneous (Cauchy medium), with a given thickness (d), a wavelength-dependent refractive index ($n(\lambda) = A + B/\lambda^2$), and a negligible extinction coefficient ($k = 0$). d and A were treated as fitting parameters, assuming $B = B_{\text{sol}}$. The χ^2 value for the best fit was typically below 2, indicating a good fit. The adsorbed oligonucleotide mass per unit area (Γ) was determined using de Feijter's equation,^{?,19}

$$\Gamma = d \cdot \frac{A - A_{\text{sol}}}{dn/dc} \quad (1)$$

with the refractive index increment of $dn/dc = 0.17 \text{ cm}^3/\text{g}$.²⁰

RESULTS AND DISCUSSION

Behavior of different anchor types. We measured the lipid-bilayer anchoring strengths of the different hydrophobic anchoring groups, Chol, C₁₈ and (C₁₈)₂ using QCM-D. A supported lipid bilayer (SLB) was formed by exposing a cleaned, silica-coated quartz crystal to a flowing suspension of small unilamellar vesicles, while monitoring the

frequency and dissipation changes of the sensor. The QCM-D response was as is expected for the formation of a SLB, see Fig. ??.^{21,22} The adsorption of the vesicles to the sensor surface is visible as a decreasing frequency and an increasing dissipation. In a second stage, the vesicles rupture and spread, signaled by an increasing frequency and decreasing dissipation. An SLB of appropriate quality is characterized by a final frequency change of $\Delta f = -25 \pm 1$ Hz and a dissipation, $\Delta D \leq 0.5 \cdot 10^{-6}$. The vesicles remaining in the bulk solution were removed by rinsing with buffer (with CaCl_2). Before the inflow of oligonucleotide suspension, the SLB was rinsed with buffer without CaCl_2 for 15 min.

We first verified that the oligonucleotide binding/unbinding is not affected by unwanted non-specific interactions. For this purpose, the QCM-D responses of unmodified oligonucleotides in contact with a SLB and of cholesterol modified oligonucleotides in contact with a bare silica coated sensor were measured. During both measurements no significant responses were detected, implying that the oligonucleotides do not exhibit any non-specific interactions with the SLB nor with the underlying silica substrate, see Fig. ?. Exploratory measurements of the binding and unbinding of Chol modified QL oligonucleotides to a SLB, indicated, however, that inter-DNA interactions on the surface can affect the DNA (un)binding, see Fig. ?. At 1 μM bulk concentrations, DINAMelt predicts a melting temperature (T_m) of roughly 0 °C for two partially hybridized QL oligonucleotides. However, if one considers a surface density of 2 pmol/cm² and a layer thickness of 10 nm (estimated from combined QCM-D and SE measurements presented in the 'Oligonucleotide organization on the surface' section), the effective oligonucleotide concentration at the surface is roughly 2000 times the bulk concentration. At 2 mM concentration, a melting temperature of about 30 °C is predicted. During the QCM-D measurements, inter-DNA interactions could hence occur. To minimize such interactions, we performed the measurements on single stranded DNA using a sequence of only thymine nucleotides.

Fig. 2a shows the QCM-D responses measured upon the introduction of the constructs QTL-Chol, QTL-C₁₈ or QTL-(C₁₈)₂ to a SLB. The resulting strong shifts in the

resonance frequency Δf and in the dissipation ΔD provide evidence for the successful formation of a soft and hydrated DNA film in all three cases. Interestingly, in Fig. 2a the adsorption kinetics for the different anchor types is substantially different. The Chol anchor incorporates the oligonucleotides the fastest into the SLB, followed by C₁₈ and finally (C₁₈)₂.

To further explore the origin of the distinct kinetics we repeated the QCM-D measurements on the samples depicted in Fig. 2a at increased flow rates of 100 and 200 $\mu\text{l}/\text{min}$. Under conditions of mass-transport limited binding, and considering the geometry of the liquid chamber (i.e. laminar flow in a slit), the adsorption rate would be expected to be linearly proportional to the cube root of the flow rate.²³ In contrast, no dependence on the flow rate would be expected if the binding process were (kinetically) limited by the insertion step into the SLB. To quantify the adsorption rates in our experiments, we numerically computed the derivative of Δf by calculating the slopes at each point in time (see for an example Fig. 3a) and plotted its minimum as a function of $\sqrt[3]{Q}$, see Fig. 3b. Next the data points were fitted with a line through the origin. The good agreement of the linear fits with the maximum absolute rates of frequency shifts depicted in Fig. 3b ($R^2 \sim 1$) shows that the maximum adsorption rates of the oligonucleotides are linearly proportional to $\sqrt[3]{Q}$ independent of anchor type. This suggests that the rate limiting step during adsorption is the transport (by convection and diffusion) of the constructs to the SLB.

As the hydrodynamic sizes of the three hydrophobically terminated oligonucleotides are similar, their respective mass transport to the surface at equal flow rate is expected to be the same, provided that the concentration of molecules available in the solution is comparable.²³ As the total oligonucleotide concentration in the measurements of Fig. 2a was kept constant, the distinct adsorption kinetics of the differently hydrophobically modified oligonucleotides may appear surprising. However, due to their amphiphilic character, the modified oligonucleotides could self-assemble into micelles in the bulk solution. The micelles would lower the concentration of free oligonucleotides in solution and would hence

impede adsorption to the SLB. Rough determinations of the critical micelle concentration (CMC) show that Chol and C_{18} modified oligonucleotides form micelles above $\sim 10 \mu\text{M}$, whereas the $(C_{18})_2$ anchor has a CMC of $\sim 1 \mu\text{M}$ (see Fig. ?? and Supplementary Information). Given a solution concentration of $1 \mu\text{M}$ in our QCM-D experiments, the $(C_{18})_2$ conjugated oligonucleotides may indeed form micelles that influence the adsorption process.

When the oligonucleotide solution was replaced by pure buffer, the frequency and dissipation responses of the sample with the Chol modified oligonucleotides were seen to return to their original level, thereby demonstrating complete desorption of the oligonucleotides from the SLB (Fig. 2a). The C_{18} conjugated strands also desorb from the SLB during rinsing, yet do not seem to come off completely within the time scale probed in the experiment. This effect could be caused by fast rebinding of the oligonucleotides to the SLB.²³ The $(C_{18})_2$ modified oligonucleotides on the other hand remain fully anchored during rinsing, which suggests that the second alkyl chain makes the hydrophobic interaction with the SLB strong enough to beat the gain in translational and conformational entropy when the oligonucleotides are freely suspended in solution.

Double versus single anchors. Having seen that the $(C_{18})_2$ conjugated oligonucleotides, which have two hydrophobic tails, bind essentially irreversibly to the SLB, we studied the impact of a second anchor on the anchoring stability of the other constructs. To this end, we hybridized two complementary oligonucleotides, QL and QLt (see Table 1) resulting in double stranded complexes of which both strands bear a hydrophobic moiety. Firstly, we investigated how the structure difference between single and double stranded oligonucleotides with a single anchor affects their adsorption and desorption to the SLB. For that purpose we hybridized the oligonucleotides QL and QLtn, creating double helices that bear only one anchor, and monitored the QCM-D responses upon interaction with a SLB. One can see in Fig. 2b that the single anchored/double stranded complexes either conjugated to Chol or C_{18} adsorb to the SLB in a qualitatively similar manner as their single anchored/single stranded counterparts. They reach maximum binding at compa-

rable rates and desorb during rinsing. Only the absolute frequency and dissipation values at maximum binding are different, indicating that the layers of oligonucleotides on the SLB are indeed differently organized. We further see that the desorption is incomplete. A possible explanation for this could be that there is a certain amount of unhybridized oligonucleotides, which could bind to other single stranded neighbors in a process that has been described in the 'Behavior of different anchor types' section. We also measured the QCM-D responses of the QL/QLtn complex conjugated to $(C_{18})_2$. Here, we again see that the single anchored/double stranded complex behaves qualitatively similar as its single stranded analog, although showing larger frequency and dissipation changes.

After confirming that double-stranded oligonucleotides display qualitatively similar behavior, we measured the adsorption kinetics and stability of double stranded oligonucleotides carrying two anchors (Fig. 2c). We find that the QCM-D responses upon rinsing with buffer show no substantial unbinding of either of the complexes, demonstrating that terminally equipping oligonucleotides with two hydrophobic moieties grants a stable binding to a SLB. Furthermore, we find that the adsorption of the double-anchored/double stranded complexes either bearing two Chol or two C_{18} groups is initially fast but gradually slows down. We hypothesize that the binding is initially mass-transport limited and then increasingly limited by surface crowding which slows down access of oligonucleotides from the solution to the surface.

Oligonucleotide organization on the surface. When the Δf and ΔD responses corresponding to the binding and unbinding of the Chol, C_{18} and $(C_{18})_2$ conjugated oligonucleotides to a SLB are plotted parametrically it can be seen that the three curves largely overlap (see Fig. 4a). The fact that the $\Delta f/\Delta D$ relations are so similar implies that the three oligonucleotide layers are similarly organized. This observation is further supported by the quantities obtained from QCM-D modeling on Δf and ΔD using the information from all overtones. From the values listed in Table 2 it becomes clear that the three oligonucleotide layers at the end of the incubation (Fig. 2a) are characterized by comparable thicknesses ($d \approx 10.5$ nm) and viscoelastic properties ($G_0' \approx 0.05$ MPa,

$G_0'' \approx 0.12$ MPa, where $G'(f) = G_0' \cdot (f/f_0)^{\alpha'}$ and $G''(f) = G_0'' \cdot (f/f_0)^{\alpha''}$ and $f_0 = 15$ MHz).

In order to relate the QCM-D frequency shifts induced by the anchorage of the hydrophobically terminated oligonucleotides to a SLB to dry mass densities, we performed simultaneous QCM-D/SE measurements. Results of the measurement of the adsorption of QTL-C₁₈ to an SLB are shown in Fig. 4b and c. Strong Δf and Γ changes directly upon injection of the oligonucleotides indicate the formation of an oligonucleotide layer on top of the SLB. In the inset, we plotted Δf vs Γ parametrically to demonstrate that Γ is approximately linearly proportional to Δf with a slope of $0.14 \text{ pmol}\cdot\text{cm}^{-2}\cdot\text{Hz}^{-1}$. This slope is subsequently used to convert Δf to Γ in all other QCM-D measurements on this particular oligonucleotide. Furthermore, because the overlapping curves in Fig. 5a suggest that the QTL oligonucleotides organize similarly on the SLB independent of the anchor, the same slope can also be used to obtain the grafting densities of the Chol and (C₁₈)₂ anchored QTL oligonucleotides.

Using the obtained grafting densities and by assuming a homogeneous distribution of hexagonally packed oligonucleotides in the SLB, we estimated the mean distance between neighboring anchors points,

$$s = \sqrt{\frac{2}{\sqrt{3}} \cdot \frac{1}{N_A \cdot \Gamma}} \quad (2)$$

where N_A is the Avogadro constant and Γ is the surface density in $\text{mol}\cdot\text{cm}^{-2}$. The pre-factor $\frac{2}{\sqrt{3}}$ represents an assumed hexagonally packed organization of the objects. The Γ and s of the oligonucleotide layers mediated by Chol, C₁₈ and (C₁₈)₂ are listed in Table 2. One can see that the spacing between the anchors in the case of Chol, C₁₈ and (C₁₈)₂ is similar to the thickness of the oligonucleotide layer. The thickness and spacing compare well with the equilibrium end-to-end distance $R_{ee} = \sqrt{2b_{nt}l_pk_{nt}}$ of ~ 13 nm of a worm-like chain of $k_{nt} = 59$ nucleotides of size $b_{nt} \approx 0.63$ nm and with a persistence length $l_p \approx 2.4$ nm.²⁴

Similarly, we determined the oligonucleotide organization of the double stranded/double

anchored oligonucleotides (QL/QLt) conjugated with Chol depicted in Fig. 2c at the moment just before rinsing. After modeling the QCM-D data and having determined the Δf -to- Γ conversion factor with combined QCM-D and SE (Fig. ??), we obtained a layer thickness of ~ 19 nm and an average oligonucleotide spacing of ~ 10 nm (Table2). Hence, the double stranded/double anchored complexes form a layer which is twice as thick as compared to the single stranded oligonucleotides, but with a comparable oligonucleotide spacing. A double stranded oligonucleotide of $k_{bp} = 47$ basepairs, when assumed as a semi-flexible rod has in solution an estimated end-to-end distance $R_{ee} = b_{bp}k_{bp}$ of ~ 16 nm with a distance between basepairs b_{bp} of 0.34 nm. The QL/QLt-Ch complex also has a 12 nucleotide overhang ($R_{ee} \approx 6$ nm) which means that the total $R_{ee} \approx 22$ nm, which is very comparable to the layer thickness as determined with QCM-D, hence the oligonucleotides anchored to the SLB are likely to be close-to-fully stretched and orientated perpendicular to the surface. Yet, regarding the estimated spacing and given a diameter of the double stranded complexes of ~ 2.0 nm there may be a certain amount of oligonucleotides that flex at their spacer, leaving them differently orientated with respect to the SLB.

Lastly, we investigated how the anchoring density is affected by the length of the oligonucleotides by performing QCM-D/SE measurements on the binding of Chol modified QTS oligonucleotides to a SLB. We determined the layer thickness of the films with QCM-D modeling to be ~ 3 nm which is a factor three thinner than the layer of the longer oligonucleotides, see Table. 2. After determining the Δf to Γ relation (Fig. ??) we found a spacing of ~ 5 nm between individual oligonucleotides. The fact that the estimated spacing between the anchoring groups is nearly twice as large as the thickness of the oligonucleotide film indicates that the DNA is not closely packed. Hence, of all the constructs measured in this study the anchoring process of the short oligonucleotide is expected to be the least affected by steric interactions with neighboring oligonucleotides. This, in combination with the complete reversibility of the binding upon rinsing and the good solubility makes the short oligonucleotide a suitable candidate for quantifying the affinity of the Chol anchor toward the SLB. To this end, we performed a QCM-D

titration measurement in which we sequentially administered increasing concentrations of oligonucleotides to a SLB, see Fig. 4. We fitted the frequency shifts at equilibrium binding for each concentration to a Langmuir isotherm,

$$\Delta f_{eq}(c) = \frac{\Delta f_{max} \cdot c}{K_D + c} \quad (3)$$

where c is the concentration of QTS-Ch in the bulk suspension and Δf_{max} is the maximally induced frequency change expected at saturation. In this way we obtained a K_D of ~ 80 nM, which is of the same order of magnitude as the 17 nM reported by Pfeiffer et al.,²⁵ who performed similar titration measurements on strands comprising twenty nucleotides at 100 mM NaCl.

CONCLUSION

Oligonucleotides can be anchored to lipid bilayers through diverse hydrophobic modifications. Here, we have investigated the binding characteristics of three frequently used anchors with the surface sensitive techniques QCM-D and SE. We find that the choice of anchor type is crucial for the stable binding of oligonucleotides to a supported lipid bilayer (SLB). Oligonucleotides conjugated to a single cholesterol (Chol) or stearyl (C_{18}) anchor were found to bind reversibly to the SLB, desorbing again upon rinsing with pure buffer. The anchoring can be enhanced by conjugating single stranded oligonucleotides to a di-stearyl ($(C_{18})_2$) anchor, or by hybridizing two Chol or C_{18} bearing oligonucleotides into double stranded complexes.

We further find that the different anchors display different adsorption kinetics. For all the anchors, the binding is limited by the transport of molecules to the substrate. However, some of the hydrophobically modified oligonucleotides may form micelles at the concentrations employed, especially the $(C_{18})_2$ anchor. Hence, it is likely that the difference in binding kinetics is caused by differences in the effective concentration of free oligonucleotides, as a result of micelle formation.

Finally, we observe that the 'long' single stranded/single anchored oligonucleotides form an equilibrium film of densely packed strands, independent of whether the binding is reversible or not. At the same bulk concentration, the double stranded/double anchored constructs, which also bind irreversibly to the SLB, form a less densely packed film. However, the lack of equilibrium binding indicates a coverage-dependent reorganization of the DNA that we attribute to the more rigid character of the double stranded helices.

The presented results on the anchoring kinetics and stability of hydrophobically modified oligonucleotides incorporated into a lipid bilayer as well as the organization of the extending oligonucleotides provide essential information for optimizing applications that require efficiently anchored, surface mobile oligonucleotides.

ASSOCIATED CONTENT

Supporting Information. Description of the critical micelle concentration determination method plus measurement results, typical QCM-D responses of the formation of a SLB, control measurements and the results of the simultaneous QCM-D and SE measurements on QL/QLt-Ch and QTS-Ch. This material is available free of charge via the Internet at <http://pubs.acs.org>.

AUTHOR INFORMATION

Corresponding Author

*E-mail: stefvandermeulen@gmail.com

ACKNOWLEDGEMENT

We thank John Randolph of Glen Research for the synthesis of the stearyl conjugated oligonucleotides and F. Huber for a critical reading of the manuscript. This work is part of the research program of the Foundation for Fundamental Research on Matter (FOM), which is financially supported by The Netherlands Organization for Scientific Research

(NWO). G. V. D. and R. P. R. acknowledge funding by the Marie Curie Career Integration Grant “CellMultiVInt” (PCIG09-GA-2011-293803) and the European Research Council Starting Grant “JELLY” (306435), respectively.

REFERENCES

- [1] Boutorin, A. S.; Gus’kova, L. V.; Ivanova, E. M.; Kobetz, N. D.; Zarytova, V. F.; Ryte, A. S.; Yurchenko, L. V.; Vlassov, V. V., Synthesis of alkylating oligonucleotide derivatives containing cholesterol or phenazinium residues at their 3'-terminus and their interaction with DNA within mammalian cells. *FEBS Lett.* **1989**, *254*, 129–32.
- [2] Shea, R. G.; Marsters, J. C.; Bischofberger, N., Synthesis, hybridization properties and antiviral activity of lipid-oligodeoxynucleotide conjugates. *Nucleic Acids Res.* **1990**, *18*, 3777–83.
- [3] Krieg, A.; Tonkinson, J., Modification of antisense phosphodiester oligodeoxynucleotides by a 5'cholesteryl moiety increases cellular association and improves efficacy. *Proc. Natl. Acad. Sci. U.S.A.* **1993**, *90*, 1048–1052.
- [4] Benkoski, J. J.; Höök, F., Lateral Mobility of Tethered Vesicle- DNA Assemblies. *J. Phys. Chem. B* **2005**, *109*, 9773–79.
- [5] Yoshina-Ishii, C.; Boxer, S. G., Arrays of mobile tethered vesicles on supported lipid bilayers. *J. Am. Chem. Soc* **2003**, *125*, 3696–7.
- [6] Yoshina-Ishii, C.; Chan, Y.-H. M.; Johnson, J. M.; Kung, L. a.; Lenz, P.; Boxer, S. G., Diffusive dynamics of vesicles tethered to a fluid supported bilayer by single-particle tracking. *Langmuir* **2006**, *22*, 5682–9.
- [7] Chan, Y.-H. M.; van Lengerich, B.; Boxer, S. G., Lipid-anchored DNA mediates vesicle fusion as observed by lipid and content mixing. *Biointerphases* **2008**, *3*, 17–21.

- [8] Beales, P. A.; Vanderlick, T. K., DNA as membrane-bound ligand-receptor pairs: duplex stability is tuned by intermembrane forces. *Biophys. J.* **2009**, *96*, 1554–65.
- [9] Chung, M.; Lowe, R. D.; Chan, Y.-H. M.; Ganesan, P. V.; Boxer, S. G., DNA-tethered membranes formed by giant vesicle rupture. *J. Struct. Biol.* **2009**, *168*, 190–9.
- [10] Chung, M.; Boxer, S. G., Stability of DNA-Tethered Lipid Membranes with Mobile Tethers. *Langmuir* **2011**, *27*, 5492–7.
- [11] van der Meulen, S. A. J.; Leunissen, M. E., Solid colloids with surface-mobile DNA linkers. *J. Am. Chem. Soc* **2013**, *135*, 15129–34.
- [12] Domack, A.; Prucker, O.; Rhe, J.; Johannsmann, D., Swelling of a polymer brush probed with a quartz crystal resonator. *Phys. Rev. E* **1997**, *56*, 680–689.
- [13] Johannsmann, D., Viscoelastic analysis of organic thin films on quartz resonators. *Macromol. Chem. Phys.* **1999**, *200*, 501–516.
- [14] Johannsmann, D., Viscoelastic, mechanical, and dielectric measurements on complex samples with the quartz crystal microbalance. *Phys. Chem. Chem. Phys.* **2008**, *10*, 4516–34.
- [15] Reviakine, I.; Johannsmann, D.; Richter, R. P., Hearing what you cannot see and visualizing what you hear: interpreting quartz crystal microbalance data from solvated interfaces. *Anal. Chem.* **2011**, *83*, 8838–48.
- [16] Eisele, N. B.; Andersson, F. I.; Frey, S.; Richter, R. P., Viscoelasticity of thin biomolecular films: a case study on nucleoporin phenylalanine-glycine repeats grafted to a histidine-tag capturing QCM-D sensor. *Biomacromolecules* **2012**, *13*, 2322–32.
- [17] Carton, I.; Brisson, A. R.; Richter, R. P., Label-free detection of clustering of membrane-bound proteins. *Anal. Chem.* **2010**, *82*, 9275–81.

- [18] Eisele, N. B.; Frey, S.; Piehler, J.; Görlich, D.; Richter, R. P., Ultrathin nucleoporin phenylalanine-glycine repeat films and their interaction with nuclear transport receptors. *EMBO Rep.* **2010**, *11*, 366–72.
- [19] De Feijter, J. A.; Benjamins, J.; Veer, F. A., Ellipsometry as a tool to study the adsorption behavior of synthetic and biopolymers at the air-water interface. *Biopolymers* **1978**, *17*, 1759–72.
- [20] Nicolai, T.; Dijk van, T. N.; Dijk van, J. A.; Smit, J. A., Molar mass characterization of DNA fragments by gel permeation chromatography using a low-angle laser light-scattering detector. *J. Chromatogr. A* **1987**, *389*, 286–92.
- [21] Keller, C., Surface specific kinetics of lipid vesicle adsorption measured with a quartz crystal microbalance. *Biophys. J.* **1998**, *75*, 1397–1402.
- [22] Richter, R.; Bérat, R.; Brisson, A., Formation of solid-supported lipid bilayers: an integrated view. *Langmuir* **2006**, *22*, 3497–3505.
- [23] Hermens, W. T.; Benes, M.; Richter, R.; Speijer, H., Effects of flow on solute exchange between fluids and supported biosurfaces. *Biotechnol. Appl. Biochem.* **2004**, *39*, 277–284.
- [24] Murphy, M.; Rasnik, I.; Cheng, W.; Lohman, T. M.; Ha, T., Probing Single-Stranded DNA Conformational Flexibility Using Fluorescence Spectroscopy. *Biophys. J.* **2004**, *86*, 2530–2537.
- [25] Pfeiffer, I.; Höök, F., Bivalent cholesterol-based coupling of oligonucleotides to lipid membrane assemblies. *J. Am. Chem. Soc.* **2004**, *126*, 10224–25.

FIGURES

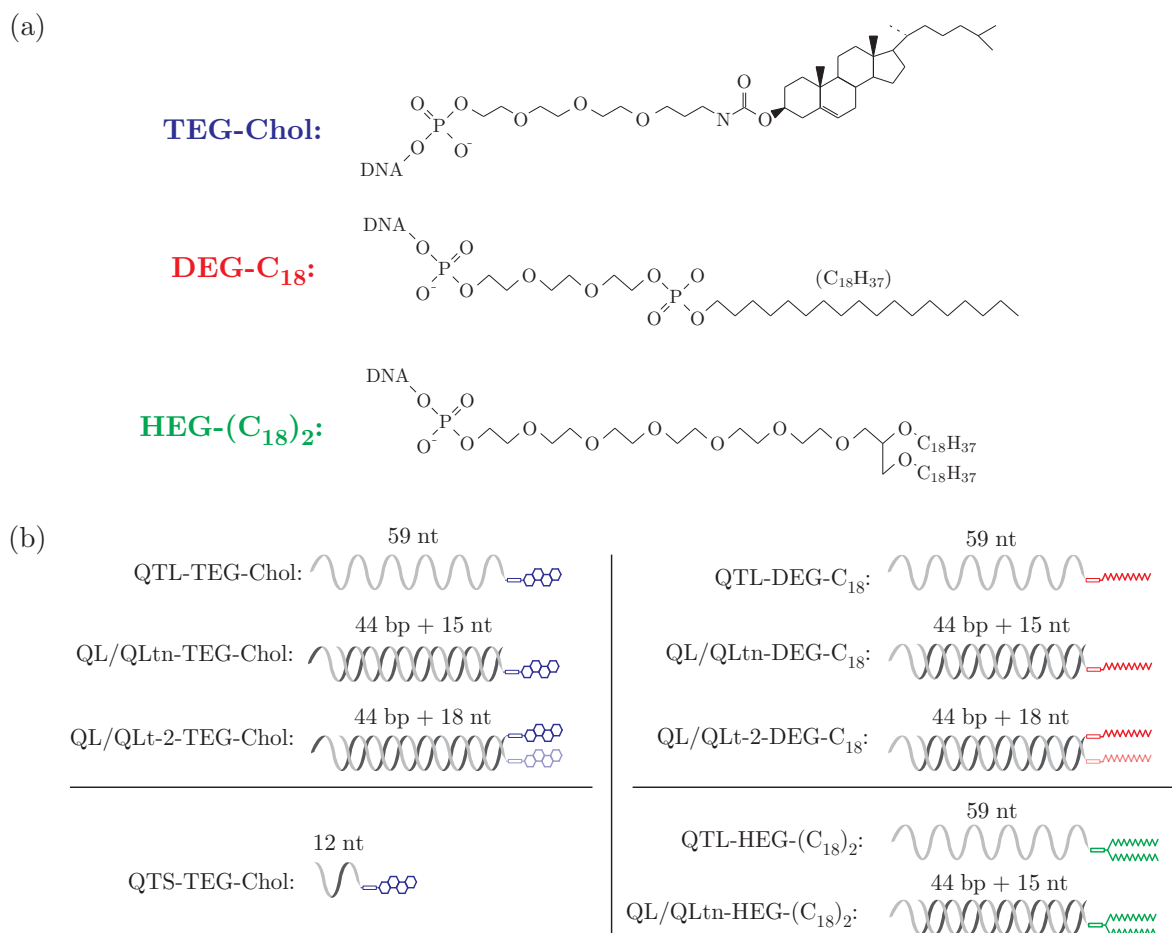


Figure 1. Oligonucleotides modified with different lipophilic moieties to anchor them to a supported lipid bilayer. (a) The three anchors: cholesterol (Chol), stearyl (C₁₈) and di-stearyl ((C₁₈)₂) are each covalently coupled to one end of the oligonucleotides through the linkers TEG = triethylene glycol, DEG = diethylene glycol and HEG = hexaethylene glycol, respectively. The positions where the oligonucleotides are coupled to the anchor are indicated by 'DNA'. (b) Schematic representations of all the complexes analyzed in this study. Each name is built out of three parts; first, the oligonucleotide sequence(s), then the linker and finally the anchor type. The number of nucleotides (nt) and basepairs (bp) are indicated above each structure.

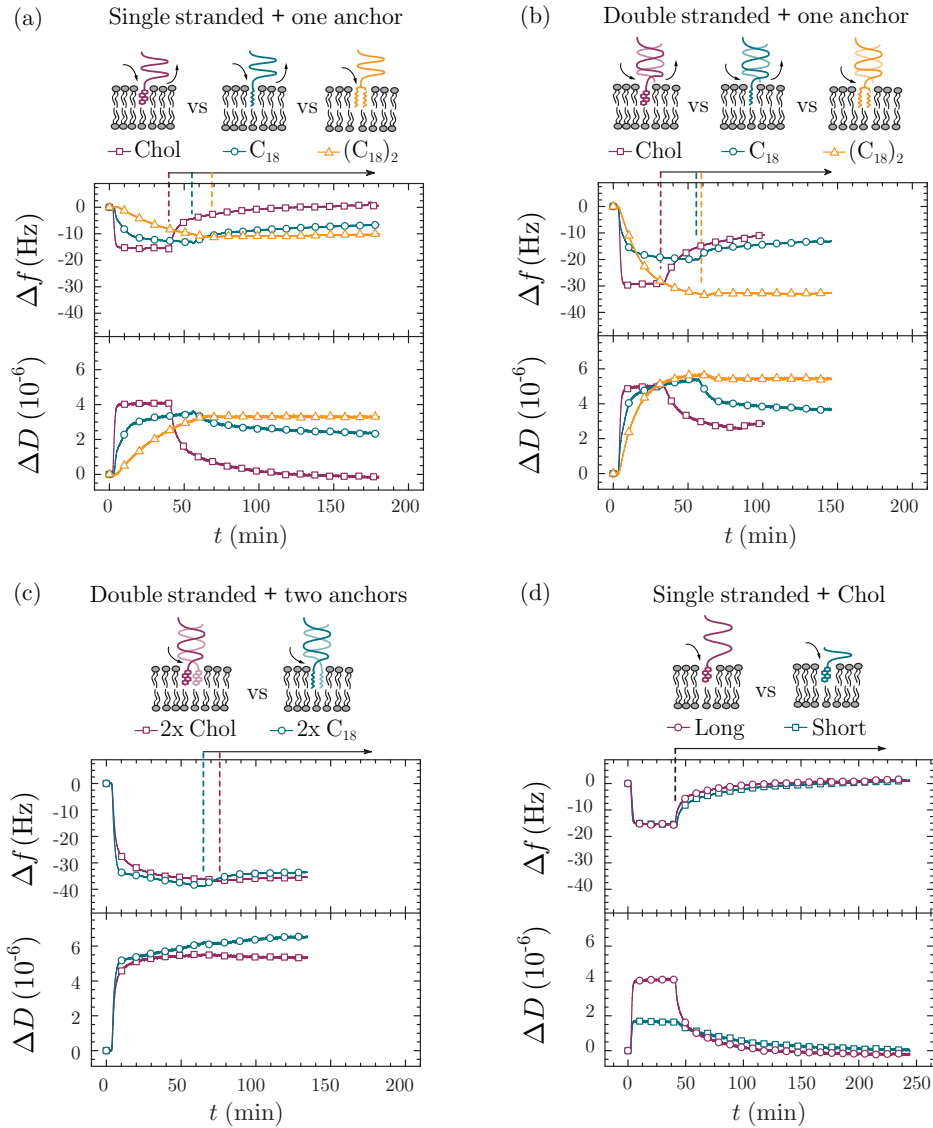


Figure 2. QCM-D measurements on the adsorption and desorption of different oligonucleotides modified with either Chol, C_{18} or $(C_{18})_2$ to a SLB. (a) The frequency Δf (top) and dissipation ΔD (bottom) changes upon exposure of a SLB to thymine-only oligonucleotides (QTL) conjugated with either Chol, C_{18} or $(C_{18})_2$ plotted as a function of time. (b) The plots of Δf (top) and ΔD (bottom) upon exposure of a SLB to double stranded complexes carrying one anchor. (c) The plots of Δf (top) and ΔD (bottom) upon exposure of a SLB to double stranded complexes carrying two anchors. (d) Plots of Δf (top) and ΔD (bottom) upon exposure of a SLB to a long (QTL) or short (QTS) oligonucleotide bearing one Chol anchor. Note that the graph corresponding to the long oligonucleotide is the same as in (a). In all measurements the oligonucleotides were injected at $t = 0$ until rinsing with buffer was initiated, which is indicated by the arrows.

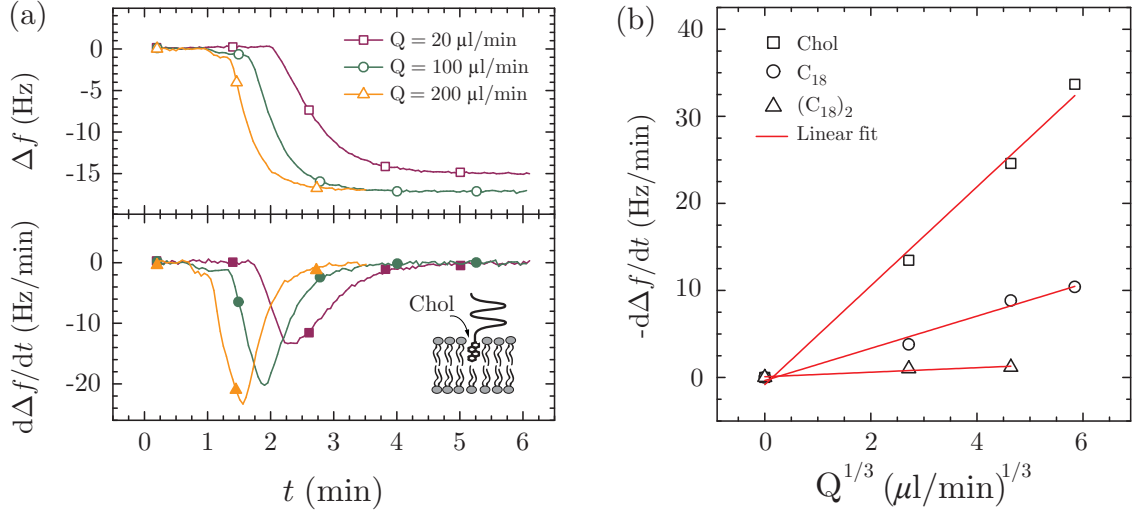


Figure 3. The flow rate dependence of the adsorption of Chol, C_{18} and $(C_{18})_2$ conjugated oligonucleotides to a SLB. (a) The frequency changes Δf (top) and their computed derivatives (bottom) during the adsorption of QTL-Chol to a SLB at different flow rates (Q) plotted as a function of time. (b) The minima of the computed derivatives shown in (a) and of the other anchors plotted as a function of $\sqrt[3]{Q}$. The plotted minima were fitted to a linear model with fixed origin at (0,0). The quality of the fits are determined by evaluating the corresponding R^2 and are found to be 0.996, 0.990 and 0.947 for Chol, C_{18} and $(C_{18})_2$, respectively.

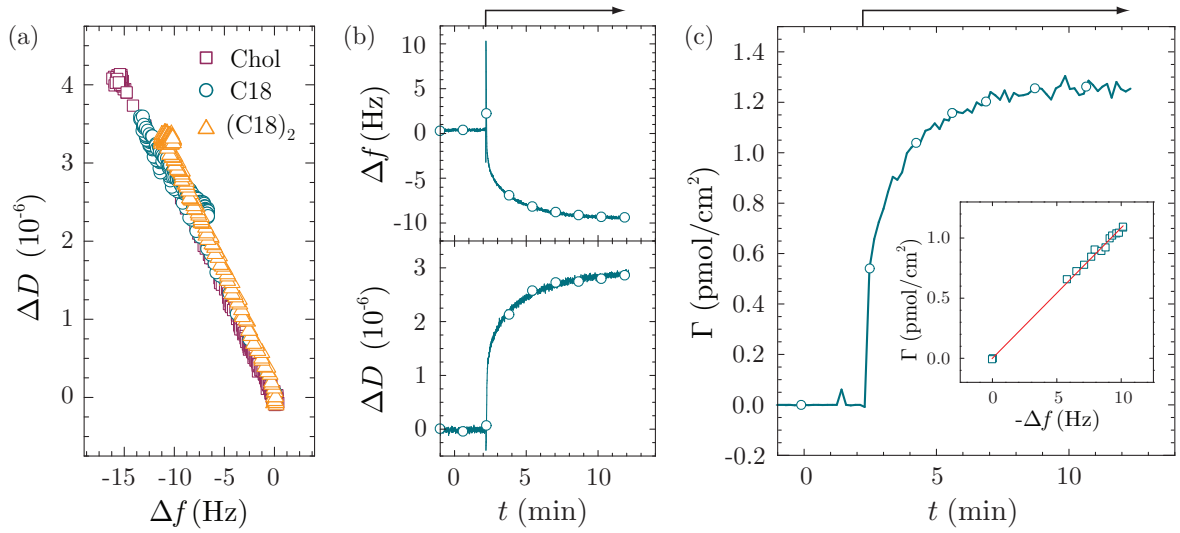


Figure 4. Determining the densities of the Chol, C₁₈ and (C₁₈)₂ conjugated oligonucleotides anchored to a SLB. (a) Parametric plots of ΔD as a function of Δf of the data depicted in Fig.2a. (b) Plots of Δf (top) and ΔD (bottom) as a function of time corresponding to the binding of QTL-oligonucleotides conjugated with C₁₈ to a SLB. Simultaneously, the surface density Γ was measured with SE as depicted in (c). The inset shows a parametric plot of Δf versus Γ , fitted to a linear model (red line) with a slope of $-0.14 \text{ pmol}\cdot\text{cm}^{-2}\cdot\text{Hz}^{-1}$. The arrows in (b) and (c) indicate the start and duration of injection.

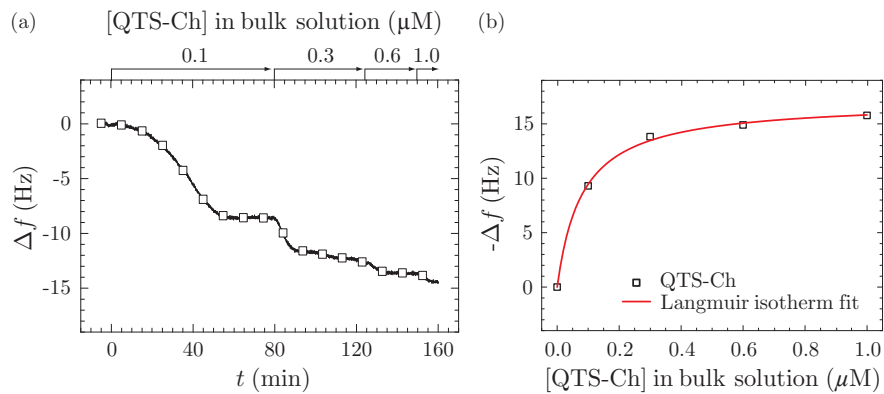


Figure 5. Anchorage of a cholesterol conjugated oligonucleotide containing 12 bases (QTS-Ch). (a) Titration curve, determined by QCM-D for the binding of QTS-Ch to a SLB. The arrows indicate start and duration of incubation with the indicated oligonucleotide concentrations to the SLB. (b) Frequency shifts (approximately proportional to adsorbed amounts) for QTS-Ch at equilibrium with a fit by a Langmuir isotherm (solid red line).

Supporting Information: QCM-D and Spectroscopic Ellipsometry Measurements of the Lipid Bilayer Anchoring Stability and Kinetics of Hydrophobically Modified DNA Oligonucleotides

Stef A. J. van der Meulen^{†,*}, Galina V. Dubacheva[‡], Marileen Dogterom^{†,§}, Ralf P. Richter^{‡,||,⊥}, and Mirjam E. Leunissen[†]

[†]FOM Institute AMOLF, Science Park 104, 1098 XG, Amsterdam, The Netherlands

[‡]Biosurfaces Unit, CIC biomaGUNE, Paseo Miramon 182, 20009 Donostia-San Sebastian, Spain

[§]Bionanoscience, TU Delft, Lorentzweg 1, 2628 CJ Delft, The Netherlands

^{||}Département de Chimie Molculaire, Université de Grenoble, BP 53, 38041 Grenoble Cedex 9, France

[⊥]Max-Planck-Institute for Intelligent Systems, Heisenbergstrasse 3, 70569 Stuttgart, Germany

*Corresponding author, E-mail: stefvandermeulen@gmail.com. Phone: +31 20 754 7284. Fax: +31 20 754 7290

EXPERIMENTAL METHODS

Detecting the CMC of hydrophobically modified oligonucleotides. A method to determine the critical micelle concentration (CMC) of surfactants is to measure the absorbance of 1-(2-pyridylazo)-2-naphthol (PAN), a water insoluble organic dye at 470 nm.¹ Below the CMC, the dye does not dissolve in the aqueous surfactant solution, and the absorbance of the solution remains low. At the CMC, a sudden rise in the solution's absorbance is observed, as the dye is encapsulated in micelles and dissolves in solution. For each compound, a titration series was prepared with final sample volumes of 450 μ l. Subsequently, 20 μ l PAN (Sigma) suspension (0.2 mg/ml dissolved in hexane) was added to each sample. The samples were vortexed and the hexane was allowed to evaporate for 30 minutes. The absorbance of each solution at 470 nm was measured using a Cary300 UV/Vis Spectrometer (Agilent, Santa Clara, CA, USA).

As a proof of principle, we determined the CMC of SDS dissolved in ultrapure water. The measured absorptions are plotted in Fig. 4. The CMC lies at around 8 mM, which is very close to the value found in the literature.² After having verified the capability of the method to detect the CMC of a common surfactant, we used this method to estimate the CMC of our hydrophobically modified oligonucleotides with sequence QL.

SUPPORTING FIGURES

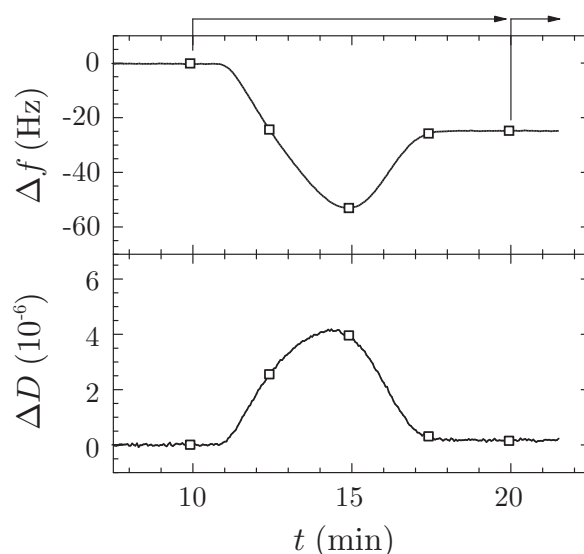


Figure 1. Formation of a supported lipid bilayer (SLB) on a silicon oxide substrate. A SLB is formed by exposing a clean silicon oxide coated sensor crystal to suspended SUVs and monitoring the crystals' Δf and ΔD responses in time. The arrows from left to right indicate the start and duration of sample administration and buffer rinsing respectively. A uniform SLB is characterized by $\Delta f \sim -25$ Hz and $\Delta D \leq 0.5 \cdot 10^{-6}$.

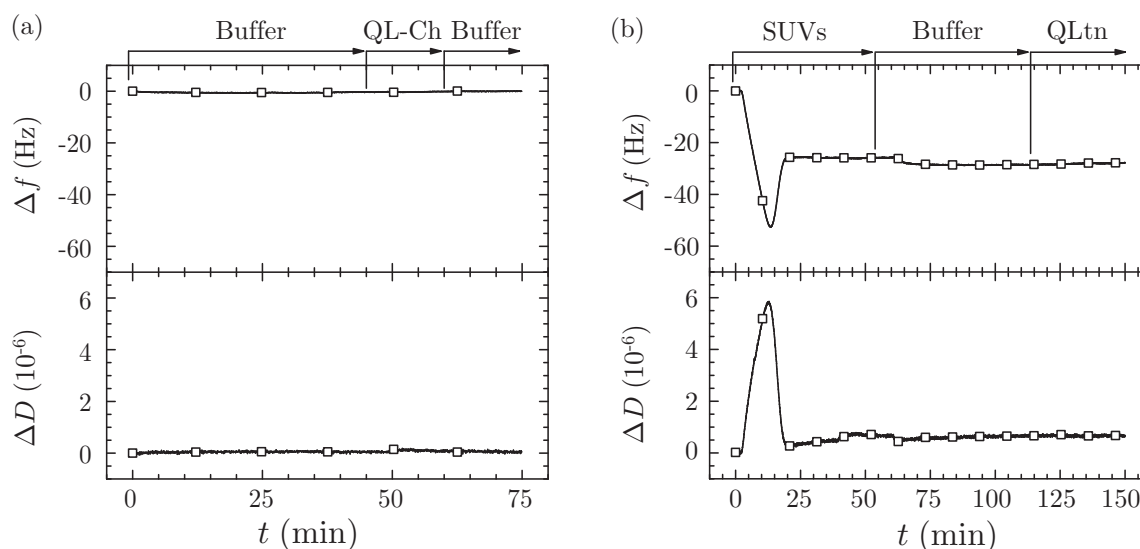


Figure 2. QCM-D measurements on the adsorption and desorption of (a) cholesterol modified oligonucleotides (QL) to a bare silica coated QCM-D sensor and (b) unmodified oligonucleotides (QLtn) to a SLB. The arrows indicate the start and duration of sample administration or buffer rinsing, as indicated.

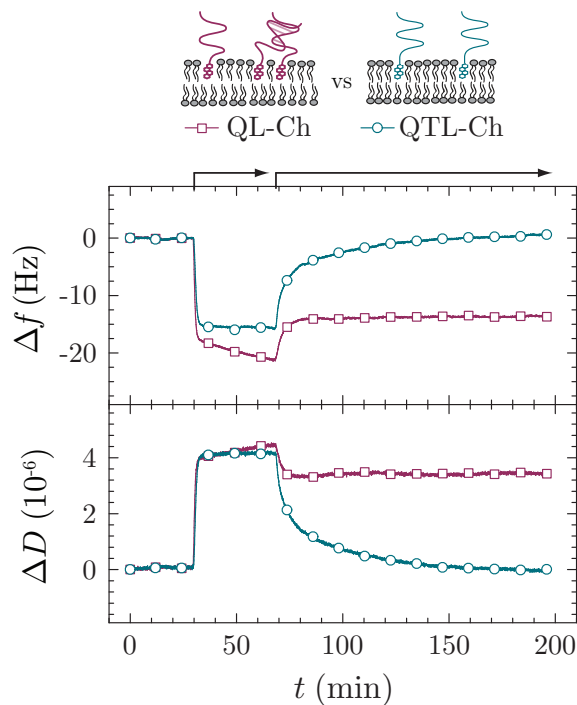


Figure 3. Comparison between the QCM-D measurements on the adsorption and desorption to a SLB of Chol-modified oligonucleotides comprising the sequence QL and the thymine-only sequence QTL. The arrows from left to right indicate the start and duration of sample administration and buffer rinsing, respectively. The incomplete unbinding of the Chol-modified oligonucleotides QL suggest that the oligonucleotides on the surface exhibit interactions between neighboring molecules. As a result, the inter-DNA interactions effectively establish double anchored constructs that stabilize their incorporation into the SLB. Using a thymine-only sequence (QTL) sufficiently minimizes the probability of inter-DNA interactions such that unperturbed unbinding is achieved.

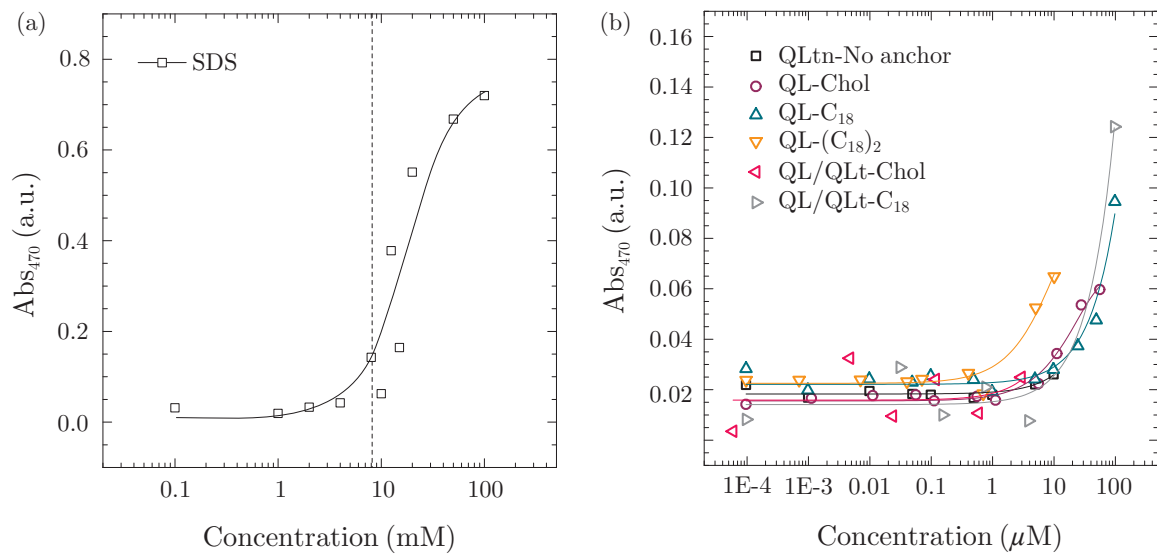


Figure 4. Detecting the CMC for hydrophobically modified oligonucleotides using UV-Vis spectroscopy. (a) Measured absorptions at 470 nm of differently concentrated SDS suspensions mixed with PAN/Hexane and ultrapure water. The solid black line is a guide for the eyes and the dashed black line indicates the CMC of SDS published in literature.² (b) Measured adsorptions at 470 nm of different concentrations of the oligonucleotides QLtn, QTL-Ch, QTL-C₁₈, QTL-(C₁₈)₂, QL/QLt-Ch and QL/QLt-C₁₈ in a solution of PAN/Hexane and buffer. The solid lines are guides for the eyes.

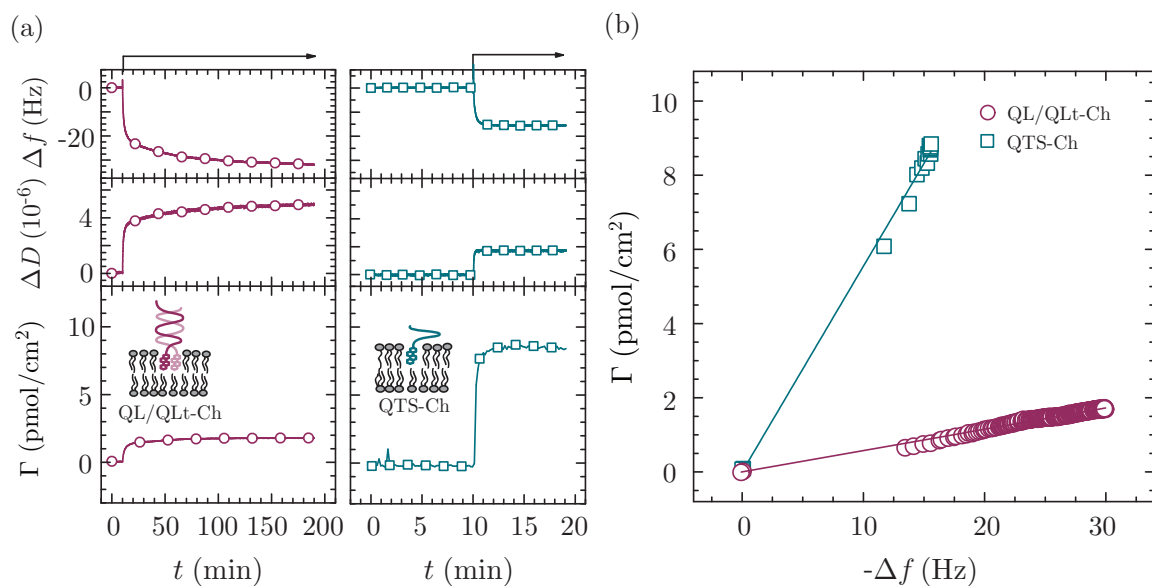


Figure 5. Determining the layer organization of QL/QLt-Ch and QTS-Ch. (a) From the top to bottom the graphs present Δf , ΔD and Γ as a function of time of the binding of QL/QLt-Ch (left) and QTS-Ch (right) to a SLB. The arrows indicate the start and duration of binding of the oligonucleotides. (b) Parametric plots of the measured Δf and Γ presented in (a). The slopes of the fits are -0.06 and -0.60 pmol \cdot cm⁻² \cdot Hz⁻¹ for QL/QLt-Ch and QTS-Ch, respectively.

REFERENCES

- [1] Nasiru, T.; Avila, L.; Levine, M., Determination of Critical Micelle Concentrations Using UV-Visible Spectroscopy. *J. High School Res.* **2011**, *2*, 1–6.
- [2] Fuguet, E.; Ràfols, C.; Rosés, M.; Bosch, E., Critical micelle concentration of surfactants in aqueous buffered and unbuffered systems. *Anal. Chim. Acta.* **2005**, *548*, 95–100.